CHAPTER 4

THEORY OF PULSAR CURRENT

4t1 INTRODUCTION

In this chapter we first outline the method of evaluating the scale factors. $S(L,P)$ which depend upon the period P and radio luminosity L of the pulsar. $S(L,P)$ is the ratio of the total number of pulsars in the Galaxy to the number detected by a pulsar survey, with the given P and L . Thus $S(L,P)$ is a 'measure of the incompleteness of a pulsar survey at the P and L . We restrict ourselves to the IIMS for reasons already mentioned in chapter 1. Next we present the theory of pulsar current J_P (PSRs Sec^{-1} Galaxy^{-1}) and discuss the qualitative features of the J_P vs. P curve. The current J_P is always a rigorous lower bound to the birthrate of pulsars; however, in a certain segment of this curve one may actually expect the birthrate itself* We compute this birthrate using a beaming fraction of 0.2 for all pulsars.

4t2 SCALE FACTORS

We compute the scale factors $S(L,P)$ using the parameters of the IIMS and the following equation for $S(L,P)$.

$$S(L,P) = \frac{\iiint \rho_{R_G}(R_G)\,\rho_z(z)\,R_G\,dR_G\,dz\,d\theta}{\iiint \rho_{R_G}(R_G)\,\rho_z(z)\,\eta(P,L,R_G,z,\theta)\,R_G\,dR_G\,d\theta\,dz} \qquad (4.1)$$

where ρ_{R_G} describes the variation of pulsar density with galactocentric radius R_G and ρ_z describes the density as a function of the height above the galactic plane* θ is the polar angle defined with respect to the galactic centre* The parameter $\eta(P,L,R_G,\theta,z)$ is set to 1 if a pulsar of period P and luminosity L at coordinates R_G , θ , z can be detected by the IIMS. Otherwise it is set to zero. Therefore the denominator of eq. (4.1) is proportional to the number of pulsars with period P and radio luminosity L which can be detected by the IIMS while the numerator is proportional to all potentially observable pulsars in the Galaxy with the same P and L . We adopted an exponential form for ρ_z with a scale height of 350 pc (Manchester 1979). For ρ_{R_G} we fitted the experimental histogram of number of pulsar against $_G$ given by Manchester (1979) to obtain the following gaussian form

$$\rho_{R_G}(R_G) \propto \mathrm{EXP}-(R_G/10.9)^2 \qquad (4.2)$$

where R_G is measured in kpc. It is interesting that the scale length of 10.9 kpc is close to the radial distance of the Sun from the galactic centre. This illustrates the well known fact that the density of pulsars falls off rapidly with galactocentric radius in the solar neighbourhood. The function in eq. (4.2) is probably incorrect in the range $0 \leqslant R_G \leqslant 4$ kpc where the observations seem to suggest a deficit of pulsars. However this region is only about 10% of the volume of the Galaxy and can cause a systematic error of at most 20% in our calculations*

$S(L,P)$ was calculated at a number of selected values of

P and L using a Monte Carlo method to evaluate the integral in eq. (4.1). The luminosities of pulsars were calculated from their radio fluxes and estimated distances; Following the convention of Taylor and Manchester (1977), we have evaluated in units of mJy.Kpc^2. Distances were calculated from the observed dispersion measures using our formula for the electron density in the Galaxy (eq.(3.17)) along with the Prentice-ter-Haar correction for HII regions within 1 Kpc of the Sun. Since this correction has significant uncertain'ties we have "damped" this correction as explained in appendix B. Wherever independently measured distances were available (Manchester and Taylor, 1981), these were used in preference*

Out of the 224 pulsars detected by the IIMS we selected a "pruned" list of 172 pulsars, The reason is that in computing $S(L,P)$ we used the published parameters (such as sensitivity, sky coverage, etc.) of the IIMS. Since the data base should also be consistent with these parameters, we have omitted those pulsars whose radio fluxes were below the minimum flux detection threshold for the IIMS. At this stage it would have been ideal to take into account the intrinsic intensity variations displayed by most pulsars* This would further affect the observability of pulsars. However this would have required detailed information such as the phase of the intensity variation of each pulsar at the time it was detected* For lack of information, we have chosen to ignore this complication*

Our Monte Carlo scheme is similar to that of Taylor and Manchester (1977), who derive an "area function" $A(R_G,L)$ for a survey; this is the effective area of the galactic plane between R_G and $R_G + dR_G$ which has been searched for pulsars of luminosity L. Thus they account for the radio luminosity selection effect by weighting the relevant functions with $A(R_G, L)$. However, they neglect the period selection effect in their calculations.

After pruning, we were left with 172 pulsars, 167 of which had measured $\dot{P}$ values* Individual scale factors were then computed for each pulsar by suitably interpolating in the matrix of $S(L,P)$ values which we had computed earlier,

4:3 THEORY OF PULSAR CURRENT

We make the following two postulates:

(1) The distribution of pulsars in the Galaxy is in a steady state* This is reasonable since the lifetime of pulsars, believed to be a few million years, is much smaller than the lifetime of our Galaxy.

(2) The period of a pulsar increases with its age* In support of this is the fact that every observed $\dot{P}$ is positive.

Let $\rho(P,\dot{P},L)dPd\dot{P}dL$ be the number of pulsars in our Galaxy in the period range P to $P+dP$, period derivative range $\dot{P}$ to $\dot{P}+d\dot{P}$, and radio luminosity range L to $L+dL$. Since $\dot{P}$ is the component of pulsar "velocity" parallel to the P-axis, the "current" of pulsars (number per unit time) at any P moving from lower values of P to higher vaues is evidently given by

$$J_p(P) = \iint \rho(P,\dot{P},L)\,\dot{P}\,d\dot{P}\,dL \qquad \text{PSRs } s^{-1}\ G^{-1} \tag{4.3}$$

It turns out that the statistics are too poor for us to compute the function J_p with any reliability from the available data. Hence we conisder an average of J_p over a range of period from P_{min} to P_{max}

$$\overline{J_p}(P_{min},P_{max}) = \frac{1}{P_{max}-P_{min}}\int_{P_{min}}^{P_{max}} J_p(P)\,dP \tag{4.4}$$

Figure 4.1 illustrates the relation between J_p and b , the birthrate of pulsars. Since all $\dot{P}$ are positive, the continuity equation implies that J_p is identically equal to the total birthrate of pulsars in the period range 0 to P , minus the deathrate in the same period range. Let all births occur between 0 and P_1 and all deaths beyond P_2 . If, as in fig. 4.1(a), $P_2 > P_1$, then there is a plateau in J_p between P_1 and P_2 where the function is equal to the total birthrate b . However* if there is an overlap of births and deaths as in fig. 4.1(b) (i.e, $P_2 < P_1$), then J_p is less than b at all P . By the above arguments, it is clear that $\overline{J_p}(P_{min}, P_{max})$ defined in eq. (4.4) is always a lower bound on b whatever P_{max} and P_{min} we may choose. In practice, we closely examine the noisy J_p calculated from the observed data and compute $\overline{J_p}$ for values of P_{min} and P_{max} selected at the edges of the apparent plateau. It is then reasonable to expect that the value of $\overline{J_p}$ so obtained is a close estimate of b itself and not just a lower bound.

The total pulsar density $\rho(P,\dot{P},L)$ is not directly available, It is related to the observed density function

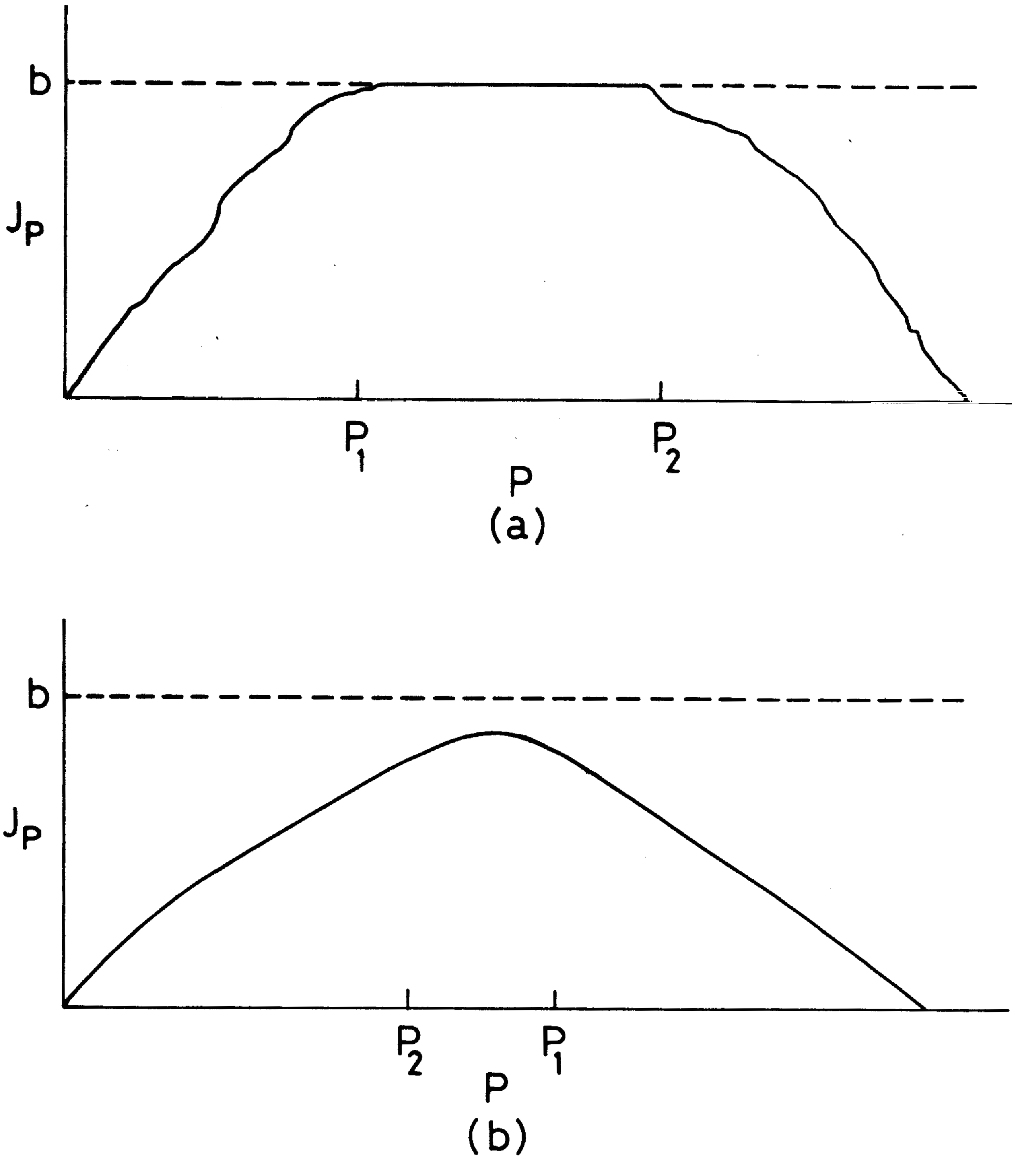

FIG. 4.1 Qualitative plot of pulsar current J_P against period P. B is the total birthrate of pulsars. All births occur for $0 < P < P_1$ while all deaths occur for $P > P_2$. Case (a): $P_2 > P_1$; Case (b): $P_2 < P_1$.

$\rho_0(P,\dot{P},L)$ by two factors: (a) There is a beaming fraction f which arises because many pulsars may not be beamed towards us.* f is generally assumed to be 0.2 (Taylor and Manchester 1977). We shall do likewise in this chapter, but in chapter 6 we discuss the possible values of in great detail. (b) There is a scale factor $S(L,P)$ which arises because pulsars of a given P and L can be detected upto a certain maximum distance by the IIMS. $S(L,P)$ also allows for the limited sky coverage of the IIMS. Therefore.

$$\rho(P,\dot{P},L) = \frac{1}{f} S(L,P)\, \rho_0(P,\dot{P},L) \tag{4.5}$$

The observed density function $\rho_Q(P,\dot{P},L)$ is not Known as a continuous function, Instead we have P, $\dot{P}$ and L values for N pulsars. We therefore approximate eq. (4.5) by the following expression

$$\rho(P,\dot{P},L) \sim \sum_{i=1}^{N} \frac{1}{f} S(L_i,P_i)\, \delta(P-P_i)\, \delta(\dot{P}-\dot{P}_i)\, \delta(L-L_i) \tag{4.6}$$

where $\delta(x)$ is the Direc delta function at $x=0$. We point out that $\overline{J}_P$ is evaluated as an integral over P, $\dot{P}$ and L and therefore the delta functions in eq. (4.6) are always integrated out in the quantities of interest to us. Substituting eq. (4.6) in eq. (4.4), we obtain an estimate of $\overline{J}_P$ in the form

$$\overline{J}_{P,est}(P_{min}, P_{max}) = \frac{(1/f)}{P_{max}-P_{min}} \sum_{i=1}^{N} S(L_i,P_i)\, \dot{P}_i ,$$

$$P_{min} \leq P_i \leq P_{max} \tag{4.7}$$

In appendix C we show that the variance of this estimator is

$$\sigma_J^2 = \frac{(1/f)^2}{(P_{max}-P_{min})^2} \sum^{N} S(L_i,P_i)\, \dot{P}_i^2 \,, \; P_{min} \leq P_i \leq P_{max} \tag{4.8}$$

*Often the beaming fraction is discussed in terms of its inverse. which is known as the beaming factor K $(= 1/f)$.

Equation (4.8) allows for errors arising from fluctuations in the observed sample but does not take into account possible errors i n . and $S(L,P)$.

As mentioned before, $\overline{J}_{P,est}$ would be an unbiased estimator of b if P_{min} and P_{max} correspond to the true plateau. region of J_P and if birth and death regions are non-overlapping as in fig. 4.1(a). If not, $\overline{J}_{P,est}$ is, in any case, an estimator of a rigorous lower bound on b .

Before closing this section we briefly discuss the convergence of the integral in eq. (4.3). Phinney and Blandford (1981) claim that (1) the observed distribution of pulsars is free from selection effects (i.e., in our notation $\rho(P,\dot{P},L)=\frac{1}{f}\langle S\rangle \rho_0(P,\dot{P},L)$ where $\langle S\rangle$ is a constant for all pulsars), (2) at large $\dot{P}$, $\rho_0 \propto \dot{P}^{-1/2}$ (3) therefore the integral in eq. (4.3) is divergent* On these grounds they expect "kinematic" approaches such as ours to be "doomed to failure" and have instead attempted a "dynamic" approach* We however find a systematic variation of $S(L,P)$ over the $P-\dot{P}$ plane (see chapter 5 for details). Therefore our scale factors ore a necessary and important input for the evaluation of the integral in eq. (4.3). Very roughly, $S(L,P)$ is seen to vary as $\dot{P}^{1/2}$. While this anticorrelation of $S(L,P)$ with $\dot{P}$ does not remove the apparent divergence noted by Phinney and Blandford, it certainly improves matters. Moreover, we show in chapter 5 that there most probably is a cutoff value of $\dot{P}$ above which pulsars apparently do not function. Such a cutoff will obviously cure all divergence problems* Finally, in the event that there really is a long tail in the distribution of pulsars at high values of $\dot{P}$, we are left with the implication that there are many unseen pulsars in the top of the $P-\dot{P}$ diagram. All results obtained from the observed sample then pertain to low P (i.e., $\dot{P} < 10^{-13}$ s/s) pulsars. If so, all forms of analysis including the "dynamical" approach, are bound to be incomplete*

4.4 NUMBER OF PULSARS IN THE GALAXY

The total number of pulsars in the Galaxy is given by

$$N_p = \iiint \rho(P,\dot{P},L)\, dP\, d\dot{P}\, dL \tag{4.9}$$

which can be written in terms of the observed ρ_0 as

$$N_p = \iiint \frac{1}{f} S(L,P)\, \rho_0(P,\dot{P},L)\, dP\, d\dot{P}\, dL \tag{4.10}$$

Using eq. (4.6) for ρ_0, we obtain the following estimate for N_p.

$$N_{est} = \frac{1}{f} \sum_{i=1}^{N} S(L_i,P_i) \tag{4.11}$$

The standard deviation σ_N of N_{est} can be shown to be given by (appendix C)

$$\sigma_N^2 = \left(\frac{1}{f}\right)^2 \sum_{i=1}^{N} S^2(L_i,P_i) \tag{4.12}$$

Using data on 172 pulsars, we obtain N_{est} to be $7.0(\pm 1.8) \times 10^5$ pulsars* Now, the error limits specified by $\pm\sigma_N$, $\pm 2\sigma_N$, etc. have well defined meanings only if the distribution of N_{est} is Gaussian. This is not so in the present case because $S(L,P)$ is spread over five orders of magnitude, The bulk of N_{est} in eq. (4.11) is actually contributed by only a few of the highest values of $S(L,P)$. We therefore expect the distribution of N_{est} to be highly asymmetric and non-Gaussian. Consequently, a more meaningful concept in the present case is the confidence limit. We have derived the following upper and lower bounds on N_{est} at a 95% confidence level (the method of calculating these confidence limits is briefly outlined in appendix D).

$$N_{est}(95\%, \text{lower}) = 4.4 \times 10^5 \tag{4.13}$$

$$N_{est}(95\%, \text{upper}) = 10.0 \times 10^5 \tag{4.14}$$

The limits in eqs. (4.13) and (4.14) are formal estimates of fluctuations arising from the poisson nature of the observed sample of pulsars, In addition, there could be significant errors in $S(L,P)$ arising from uncertainties in distances to pulsars and in , Arnett and Lerche (1981) have in fact concluded that uncertainties in n_e and f are so large that any statist'ical analysis of pulsar data is meaningless, We, however, take a more optimistic view, Nevertheless, we emphasize that systematic uncertainties of the kind mentioned above could very well be as large as the statistical uncertainties.

Our results are in good agreement with the currently accepted value (Taylor and Manchester 1977) of $N_p \sim 5 \times 10^5$. This is an independent check on our analysis and, in particular, on our values of $S(L,P)$,

4.5 PULSAR BIRTHRATE

We estimate the birthrate by the "plateau" value of $\overline{J}_{P,est}$ as described in section 4.2. Figure 4.2 shows the values of $\overline{J}_{P,est}$ in three period bins. This bin size was selected so as to have the best combination of good resolution in period and good error estimates (each bin has $\sim$ 55 pulsars). It would appear from fig. 4.2 that a plateau exists from P_{min} =0.4502 s. to P_{max} =0.8268 s. We thus estimate the birthrate of pulsars to be

$$b \sim \overline{J}_{P,est}(0.4502, 0.8268) = 0.08^{+0.07}_{-0.04} \quad \text{PSRs } s_{\cdot}^{-1}\, G.^{-1} \qquad (4.15)$$

or one pulsar born every 13^{+17}_{-6} yrs , where the error bounds represent the 95% confidence limits. The above result is slightly different from, but consistent with, the value we had published earlier (Narayan and Vivekanand 1981). The difference arises because P_{min} was earlier taken to be 0.0 s.

There are two noteworthy features of our calculation. Firstly, it is independent of any model for pulsar evolution, whereas all (but one!) previous calculations assumed a model. Secondly, our calculation is the first to incorporate the radio-luminosity and period selection effects. Phinney Blandford (1981) did use a model independent approach, but did not incorporate the selection effects, Thus our value for the birthrate may be the most reliable number available so far, We will discuss the. implication of our birthrate estimate in chapter 8.

4.6 BIRTHRATE ON THE BASIS OF THE DIPOLE BRAKING MODEL

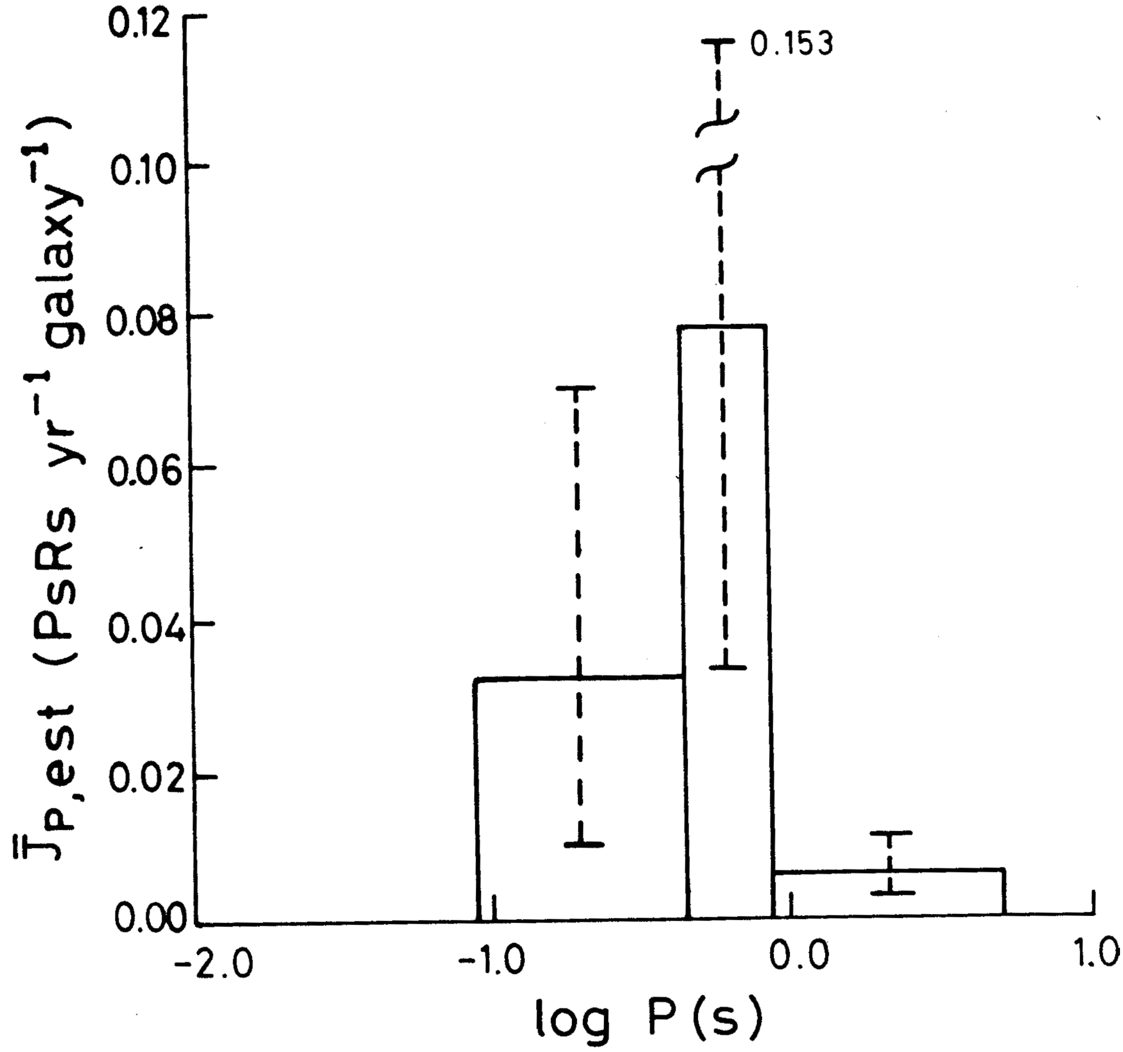

FIG.4.2 Plot of estimated mean pulsar current $\bar{J}_{P,est}$ against period P. Each bin contains approximately 55 pulsars. Error limits are specified at a 95% confidence level. JP has been averaged over the relevant period intervals. However, the qualitative nature of the histogram remains unchanged under finer binning in period. Scale values S(L,P) (derived from observed luminosities) have been used.

We discuss a modification of our theory which permits us to estimate the birthrate assuming the dipole braking model of pulsar evolution*

Let $\rho_0(\tau, L)$ be the observed density of pulsars with radio luminosity between L and $L+dL$ and age τ $(=\frac{1}{2}P/\dot{P})$ between τ and $\tau+d\tau$. If is the age, then the "velocity" of pulsars along the τ-axis is $\dot{\tau}=1$. Therefore, the current J_τ of pulsars at an age τ parallel to the τ-axis is given by

$$J_\tau(\tau) = \int \frac{1}{f} S(L,P)\,\rho_0(\tau,L)\,dL \qquad (4.16)$$

As before J_τ is equal to the birthrate of pulsars in the age range 0 to τ minus the deathrate in the same range of age, Once again, for better statistics, we average J_τ from τ_{min} to τ_{max}.

$$\overline{J_\tau}(\tau_{min},\tau_{max}) = \frac{(1/f)}{\tau_{max}-\tau_{min}} \int_{\tau_{min}}^{\tau_{max}} J_\tau(\tau)\,d\tau \qquad (4.17)$$

An estimator of this quantity is

$$\overline{J}_{\tau,est}(\tau_{min},\tau_{max}) = \frac{(1/f)}{\tau_{max}-\tau_{min}} \sum_{i=1}^{N} S(L_i,P_i)\,, \quad \tau_{min} \le \tau \le \tau_{max} \qquad (4.18)$$

Equation (4.18) is similar to the birthrate formula of Davies, Lyne and Seiradakis (1977) except that we use individual scale factors for the pulsars and also introduce τ_{min}, which is 0 in their case.

In fig. 4.3 we have shown $\overline{J}_{\tau,est}$ in "equal-number" bins of the age, Since the error bars are large it is difficult to locate the plateau region with great confidence, If we take the

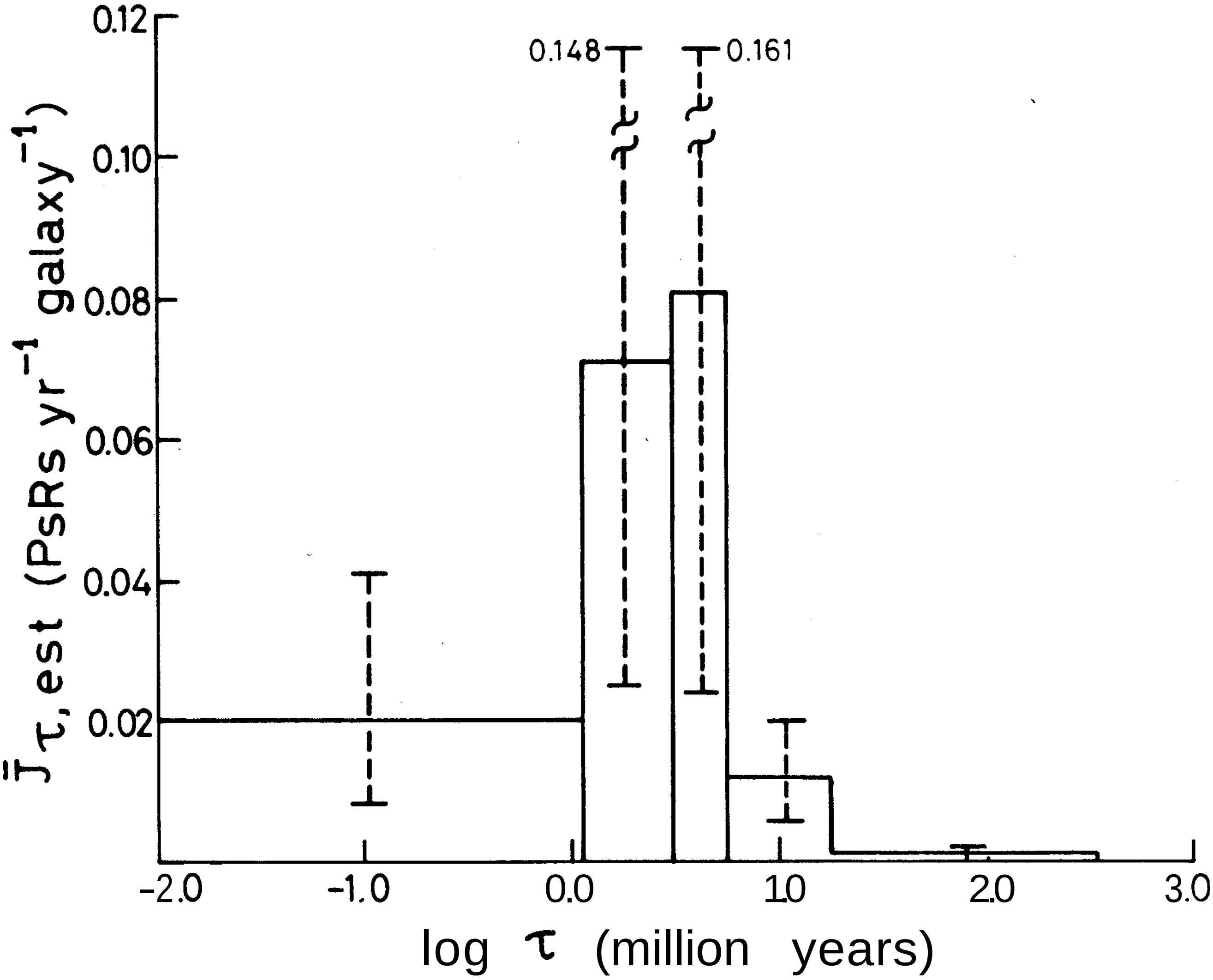

FIG.4.3 Plot of estimated mean pulsar current $\bar{J}_{\tau,est}$ against apparent pulsar age $\tau = \frac{1}{2}P/\dot{P}$. Each bin contains approximately **33** pulsars. J_τ has been averaged over the relevant age intervals. Error limits are specified at a 95% confidence level. J, definitely drops from the first to the fourth bin, although J, in the second and third bins is not determined clearly. There is no detectable change in J_τ for bins of higher apparent ages. Scale values S(L,P) have been used.

plateau to extend from 0 to 6 million years, we obtain a birthrate of 0.04 pulsars yr^{-1} $Galaxy^{-1}$, or one pulsar every 25^{+45}_{-14} years. This is consistent with the result of the previous section, suggesting that young pulsars may'be evolving accordinq to the dipole law. Figure 4.3 shows a significant drop in the value of $\overline{J}_{\tau,est}$ after 6 million years. This suggests that beyond 6 million years either pulsars could be dying or the relation age $= \frac{1}{2} P/\dot{P}$ may no longer be valid (say, due to magnetic field decay).

4.7 IMPORTANCE OF RADIO LUMINOSITY SELECTION EFFECTS

Are the radio luminosity and the period selection effects important for the computation of the birthrate? We can answer this question by comparing the birthrate in section 4.5 with a second calculation where all pulsars are weighted equally with an average scale factor $\langle S \rangle$, Equation (4.7) would then become

$$\overline{J}_{P,est}(P_{min},P_{max}) = \frac{(1/f)\langle S \rangle}{P_{max}-P_{min}} \sum_{i=1}^{N} \dot{P}_i \;, \quad P_{min} \leq P_i \leq P_{max} \qquad (4.19)$$

We have made a thorough statistical comparison of the currents calculated by eq. (4.7) and (4.19) on the basis of which we can say with greater than 80% confidence that the two quantities are not the same. We are therefore quite certain that "radio luminosity" as well as "period" selection effects are too important to be neglected*

CHAPTER 5

INJECTION

5.1 INTRODUCTION

In this chapter we discuss a very important result of our analysis, We see in fig. 4.2 that $\bar{J}_{P,est}$ appears to be significantly higher in the second bin compared to the first. It is clear that such a situation can arise only if some pulsars make their appearance in bin 2 without flowing through bin 1. In other words, some radio pulsars are apparently "born" in the period range ~ 0.45 s. to ~ 0.83 s. We have named this phenomenon "injection" of pulsars and have verified that it is not dependent on the particular choice of the bin sizes. It is however, not possible to have a more detailed look at injection given the present level of noise on $\bar{J}_{P,est}$ in fig* (4.2). Our basic attempt in this chapter is to reduce the statistical errors on $\bar{J}_{P,est}$ Now, the high variance on $\bar{J}_{P,est}$ is on account of the large ($\sim$ five orders of magnitude) spread in the values of the scale factors, which is in turn caused by a similar spread in the observed radio luminosities* In this chapter we derive'new scales whose variance- is smaller, This we achieve by modelling the dependence of the radio luminosity upon P and $\dot{P}$. We thus derive a "mean" luminosity L' which has a "smooth" dependence upon P and $\dot{P}$, in contrast to the old

L values, Furthermore, we allow for the fact that, at a given P and $\dot{P}$, there is a distribution of L around L'. Using this distribution we calculate mean scale values $s'(P,\dot{P})$ at any P and $\dot{P}$. The scatter in the new scales is reduced from five to three orders of magnitude* Consequently, there are much smaller statistical errors in the new estimates of the birthrate and other quantities. However it must be kept in mind that the entire analysis in this chapter is critically dependent upon the luminosity model.

5.2 MODEL FOR LUMINOSITY CORRELATIONS

We fitted a least squares plane to the data of $\log L$ against $\log P$ and $\log \dot{P}$ for the 167 "pruned" pulsars from the IIMS to obtain the mean luminosity L' in the following form

$$L'(P,\dot{P}) \propto P^{-0.9(\pm 0.2)}\ \dot{P}^{+0.5(\pm 0.1)} \qquad (5.1)$$

where the numbers in the brackets represent 1σ errors, computed in the usual way for correlated parameters, Lyne, Ritchings and Smith (1975) did a similar exercise and obtained $L' \propto P^{-1.8}\dot{P}^{0.9}$, However they did not fit a least squares plane but instead arrived at their result by maximizing a correlation coefficient between L and a known function of P and $\dot{P}$. This may explain the discrepancy between their result for the exponents and ours. To check this we fitted a least squares plane to the data of 84 pulsars used by them and obtained $L' \propto P^{-0.8}\dot{P}^{+0.4}$ which is consistent with our result in eq. (5.1).

We now make the crucial approximation that the observed density distribution of pulsars $\rho_0(P,\dot{P},L)$ can be separated into the product of two functions in the form

$$\rho_0(P,\dot{P},L) = \rho_1(P,\dot{P})\,\rho_2(\log L - \log L') \qquad (5.2)$$

where ρ_1 is the density of pulsars in the $P-\dot{P}$ plane, ρ_2 is normalised to 1 and $L'(P,\dot{P})$ is defined in eq. (5.1). We are thus assuming that the distribution of $\log L$ is the same at all points in the $P-\dot{P}$ plane except for the shift given by $\log L'(P,\dot{P})$. We have made the following statistical test of this hypothesis. We divided the $P-\dot{P}$ plane into four quadrants, each containing approximately the same number of pulsars, In each quadrant we separately tabulated the values of $(\log L - \log L')$ of the observed pulsars. Taking five bins in this variable we carried out a -test to verify that the distributions in the four quadrants are the same. We obtained a χ^2 value of 22.0 while the number of degrees of freedom of tho test is 12.0. However, a closer look at the distributions in each of the four quadrants showed that only one bin, viz., the bin containing the highest luminosity pulsars in the "short P-high $\dot{P}$" quadrant, was responsible for the major fraction of the χ^2. Now five out of the six pulsars in this bin have large dispersion measures (DM) 280 pc cm^{-3}). All of these lie within 60^o of longitude from the galactic centre except one, which lies within 20^o degress. We feel that the computed distances to most of these pulsars (and therefore their luminosities) must be significantly overestimated because of unaccounted HII regions along the line of sight. We have repeated the entire model-fitting calculation after removing altogether two pulsars from this bin (PSR 1641-45 and PSR 1240-64), and obtained a χ^2 of 18.0, which is a significant improvement* If these pulsars were not removed but their luminosities were reduced by, say, a factor of 2 (which is a reasonable error in pulsar luminosities due to uncertainties in their distances), the χ^2 would improve further* We performed this test on an enlarged sample of 242 pulsars which included pulsars from the Arecibo survey and the Jodrell Bank survey as well In this case we obtained a χ^2 of 13.6 against the expected value of 12.0. We therefore take the stand that eq. (5.2) is an unbiased representation of the pulsar sample. Needless to say, results derived on the basis of this model must be treated with a lot of caution.

Equation (5.2) can be written in the equivalent form

$$\rho_0(P,\dot{P},L) = \rho_1(P,\dot{P})\,\rho_2'(L/L'(P,\dot{P})) \qquad (5.3)$$

where again ρ_2' is normalised to 1. The mean scale factor $S'(P,\dot{P})$ at a given (P , $\dot{P}$) is then obviously given by

$$S'(P,\dot{P}) = \int_0^\infty \rho_2'(L/L'(P,\dot{P}))\,S(L,P)\,dL \qquad (5.4)$$

where $S(L,P)$ is the old scale factor defined in chapter 4. $S'(P,\dot{P})$ can be approximately calculated in terms of the data on 167 pulsars by means of the expression

$$S'(P,\dot{P}) = \frac{1}{167}\sum_{i=1}^{167} S(\xi_i(P,\dot{P}),P) \qquad (5.5)$$

where

$$\xi_i(P,\dot{P}) = L'(P,\dot{P})\,L_i\,/\,L'(P_i,\dot{P}_i) \qquad (5.6)$$

We have computed $S'(P_i,\dot{P}_i)$ for each of the 167 pulsars in the pruned list and used these in the calculation's described in the rest of this chapter*

To summarize, in this section we calculate the scale factor of a pulsar, not in terms of its observed luminosity but in terms of the expected distribution of its luminosity at a particular value of P and At the heart of this approximation is the basic assumption (eqs. (5.1) and (5.2)) that the luminosity distribution is the same at all P and $\dot{P}$ except for the scaling by $L'(P,\dot{P})$. Although our statistical test had produced rather large χ^2, we are certain that only two, or at the most three pulsars are responsible for this.

5.3 PULSAR BIRTHRATE

Using the new scales eq. (4.7) becomes

$$\overline{J'_{P,est}}(P_{min}, P_{max}) = \frac{(1/f)}{P_{max}-P_{min}} \sum_{i=1}^{N} S'(P_i,\dot{P}_i)\,\dot{P}_i\,, \quad P_{min} \leq P_i \leq P_{max} \qquad (5.7)$$

We have plotted $\overline{J'_{P,est}}$ in fig* 5.1. Comparison with fig. 4.2 shows that the new scales have significantly improved the error limits* The plateau appears to extend from ~ 0.45 s. to ~ 0.83 s. The mean value of $\overline{J'_{P,est}}$ in this range is $0.063^{+0.017}_{-0.016}$, giving a birthrate of one pulsar every 16^{+3}_{-5} years in the Galaxy. This is consistent with the number derived in chapter 4, but has much smaller error limits. However, ae will treat this number with caution for two reasons* Firstly, it is based on the radio luminosity model which may or may not be accurate* Secondly, this number is directly proportional to ($1/f$) Inthe next chapter we will discuss the nature of f in great detail.

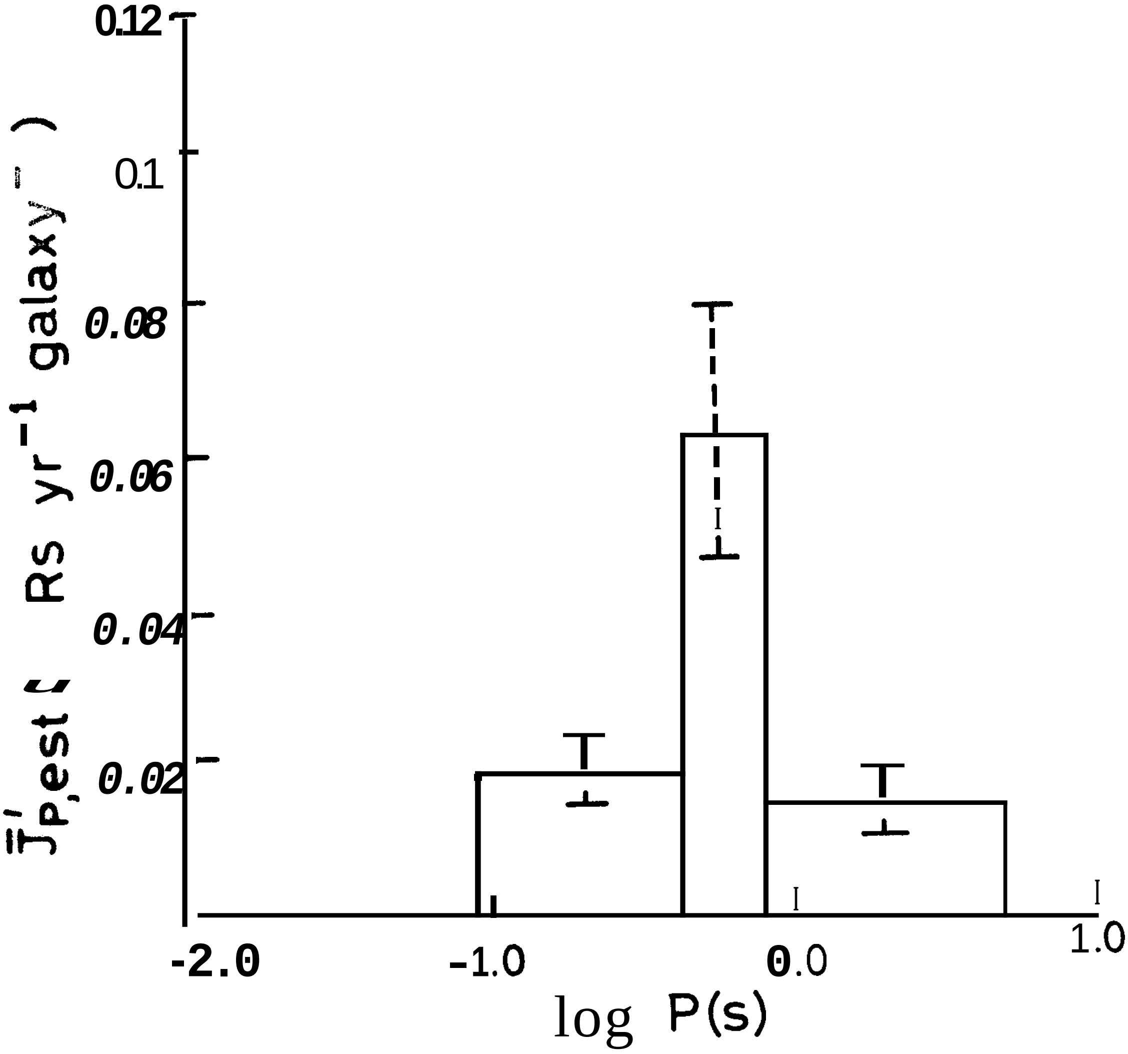

FIG. 5.1 **Same** as in Fig. 4.2, but with improved scale values S'(P,Ṗ) derived from P and Ṗ. J_p increases in the second bin and drops significantly in the third bin, closely following Fig. 4.1(a).

5.4 INJECTION

In order to understand the details of injection, we have subdivided each bin in fig* 5.1 into three further bins in $\dot{P}$. The estimated mean current $\overline{J'}_{P,est}$ in the various bins are shown in table 5.1, along with the 95% confidence limits. There seems to be strong evidence that injection occurs at high values of $\dot{P}$ in the period range - 0.5 s to ~1.0 s. We have outlined this high injection region by means of the box in fig* 5.2.

The injected pulsars are unlikely to be the "recycled" pulsars formed in massive close binary systems (de Loore, de Greve and de Cuyper 1975), because there is no compelling reason to expect predominantly high values of $\dot{P}$ in such pulsars. On the contrary, low values of are likely to occur if magnetic fields of pulsar decay on the time scales of $\sim 5\times10^{6}$ years, which is the estimated time between the two explosions. Injection, on the other hand, occurs at high values of $\dot{P}$.

We have two possible explanation to offer for injection'

(1) It is likely that neutron stars are born with initial periods ranging right from milliseconds to one second. Small values for the initial period are easily obtained if a major fraction of the angular momentum of the pulsar progenitor is conserved by the neutron star; and large values of initial period are obtained if the angular momentum is lost either before or during the collapse into a neutron star, or soon after, say, by the mechanism of gravitational radiation. We point out, however, that Manchester and Taylor (1977) have

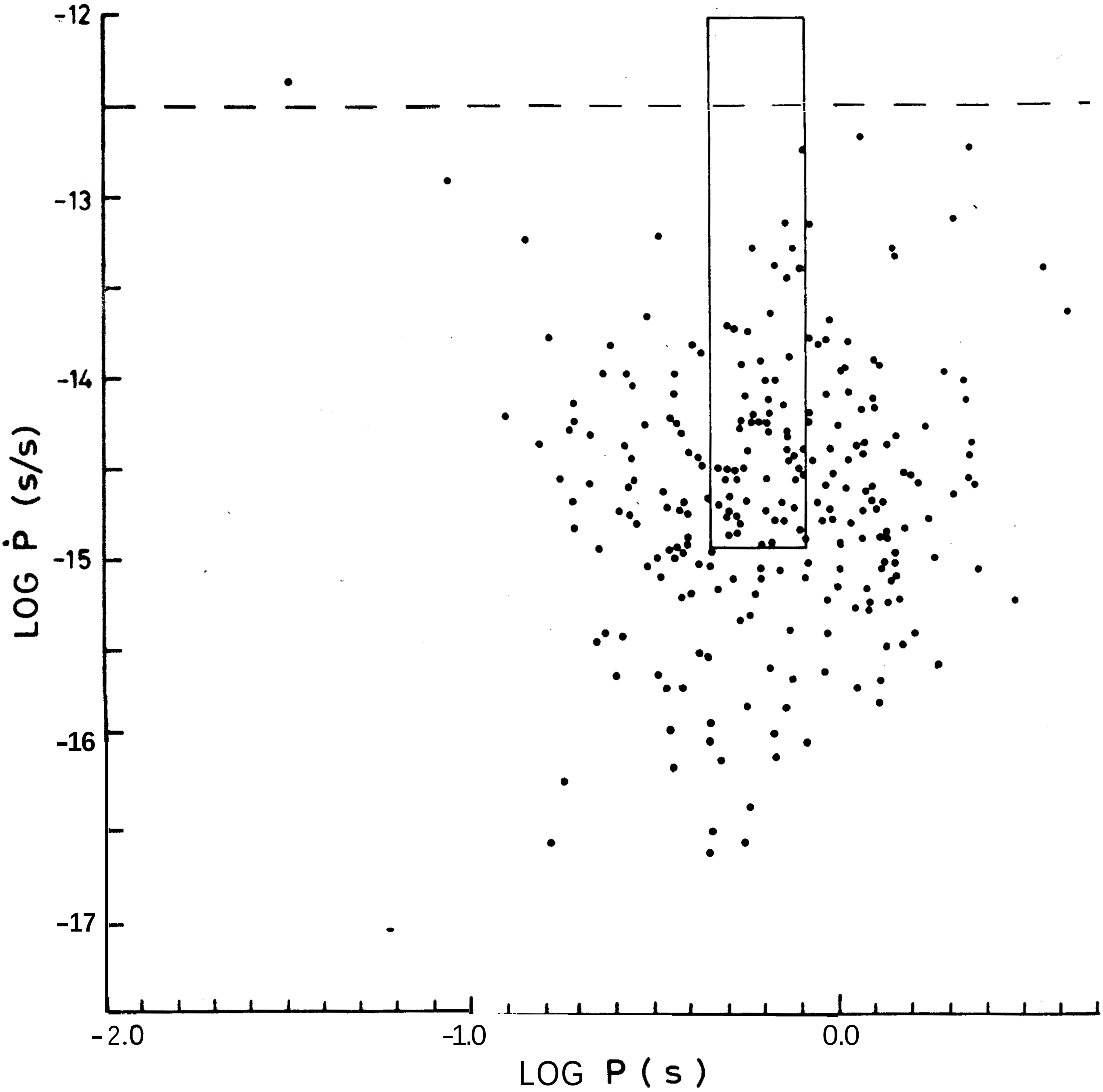

FIG. **5.2** Periods and period derivatives plotted on log-log scale for 256 pulsars. Pulsars appear to be missing above a critical value of Ṗ, tentatively represented by the dashed "cut-off" line. Pulsars are born in the top left part of the diagram (the majority being born apparently above the cut-off line), and evolve towards the bottom right of the diagram. Most of the pulsar injection occurs in the box at the top of the diagram.

TABLE 5.1

Estimated mean pulsar current $\overline{J'_{P,est}}$ in various bins of the $P - \dot{P}$ diagram. The 95% upper and lower limits to the currents are also specified in the important bins. P is in units of seconds and $\dot{P}$ is in units of 10^{-15} seconds per second.

	$0.0 \leq P < 0.45$	$0.45 \leq P < 0.83$	$0.83 \leq P < 3.00$
$4.2 \leq \dot{P}$	$0.008^{+0.004}_{-0.004}$	$0.033^{+0.013}_{-0.013}$	$0.013^{+0.005}_{-0.005}$
$1.3 \leq \dot{P} < 4.2$	$0.006^{+0.003}_{-0.003}$	$0.020^{+0.008}_{-0.007}$	$0.007^{+0.003}_{-0.003}$
$\dot{P} < 1.3$	$0.005^{+0.002}_{-0.002}$	$0.009^{+0.003}_{-0.003}$	$0.004^{+0.002}_{-0.002}$

argued that no mechanism exists for the progenitor to lose its angular momentum*

(2) If, for some reason, all neutron stars are born spinning rapidly, then the absence of high $\dot{P}$ pulsars in fig. 5.2 suggests another explanation for injection. A close examination of this figure shows that there is apparently an abrupt cut-off of pulsars above a certain value of $\dot{P}$ We have made the following statistical test to determine whether the scarcity of pulsars at high $\dot{P}$ is indeed significant. We tentatively placed the cut-off line at $\log \dot{P} = -12.5$ (fig. 5.2). We assumed a dipole braking model without field decay (which is reasonable for this part of the $P-\dot{P}$ diagram), and a pulsar death line of the form $\dot{P} P^{-5}$ =const. (Ritchings (1976) has shown that at small values of $\dot{P} P^{-5}$ pulsars spend increasing lengths of time in the nulled state, apparently as a prelude to death). Assuming the period at birth to be 10 ms, we computed the birthrate of pulsars in various bins of $\dot{P}$ using the observed sample of pulsars and the scale factors $S'(P,\dot{P})$. We then evolved the pulsars according to the dipole braking law and computed the number of pulsars we should have observed above the cut-off line. This turns out to be 11.1 pulsars* Since some of these might have been missed by the IIMS due to their having very low periods, we also computed the expected number of pulsars above the cut-off line with $P > 100$ ms. Our calculations show that we should have seen 4.7 pulsars, whereas we see only one (which is the recently discovered pulsar PSR 1509-58 in MSH 15-52), We have verified that the above results are not very sensitive to the exact location of either the cut-off line or the death line* At this stage we again emphasise that these

calculations depend critically upon the validity of the luminosity model which we have assumed* Therefore we restrict ourselves to deriving from the above result only the qualitative inspiration that there, could be a deficit of pulsars at large values of $\dot{P}$.

We offer the following explanation for injection* It is possible that neutron stars do not radiate in the radio region immediately after birth, but do so later in their lives* We suggest that neutron stars with $\dot{P}$ greater than a critical. value are unable to radiate in the radio* They switch on as pulsars when their P decays to the critical value. Therefore neutron star with P greater than the critical value will enter the P-$\dot{P}$ diagram at higher periods, thereby giving rise to injection* At present we have no theory to explain the cut-off line in the P-P diagram,

The above scenario also helps to explain why there are so few pulsar-supernova remnant associations, Our data suggests that pulsars could spend $\sim$50,000 years above the cut-off line, Since there is good evidence that supernova remnants dissolve into the interstellar medium on such time scales, there would be very few observable associations between these two species* However, in this picture we also require that neutron stars cool rapidly after birth to avoid radiating thermal x-rays because hot neutron stars would surely have been detected within the known supernova remnants with the presently available satellite instruments*

5.5 BRAKING INDEX

The braking index n is defined by the equation

$$\dot{\Omega} \propto \Omega^{-n} \tag{5.8}$$

where the angular velocity $\Omega = 2\pi/P$, In the dipole braking theory, $n=3$, The age τ of a pulsar, assuming the initial period to be 0 s, can be expressed in terms of the braking index as

$$\tau = \frac{1}{(n-1)} \frac{P}{\dot{P}} = \frac{\tau'}{(n-1)} \tag{5.9}$$

where τ' is the characteristic time $P/\dot{P}$, The velocity of a pulsar parallel to the τ' -axis is $\dot{\tau}' = (n-1)$. Hence the mean pulsar current along this axis can be written, as in earlier sections, as

$$\overline{J}_{\tau',est}(\tau'_{min},\tau'_{max}) = \frac{(1/f)}{\tau'_{max}-\tau'_{min}} \sum_{i=1}^{N} (n_i-1)\, S'(P_i,\dot{P}_i) ,$$

$$\tau'_{min} \le \tau' \le \tau'_{max} \tag{5.10}$$

If we define $\langle n\rangle$ as the mean braking index of the pulsars in the τ' range' defined in eq. (5.10), then the equation can be written as

$$\overline{J}'_{\tau',est}(\tau'_{min},\tau'_{max}) = \frac{(1/f)(\langle n\rangle-1)}{\tau'_{max}-\tau'_{min}} \sum_{i=1}^{N} S'(P_i,\dot{P}_i)$$

$$= (\langle n\rangle-1)\, X(\tau'_{min},\tau'_{max}),$$

$$\tau'_{min} \le \tau' \le \tau'_{max} \tag{5.11}$$

We have plotted $X(\tau'_{min},\tau'_{max})$ in bins of 2 million years in fig, 5.3. The curve appears to be essentially constant up to 12 mil lion years, and fal ls thereafter, If we assume the dipole model and take the age as $\tau'/2$, then it would appear that upto

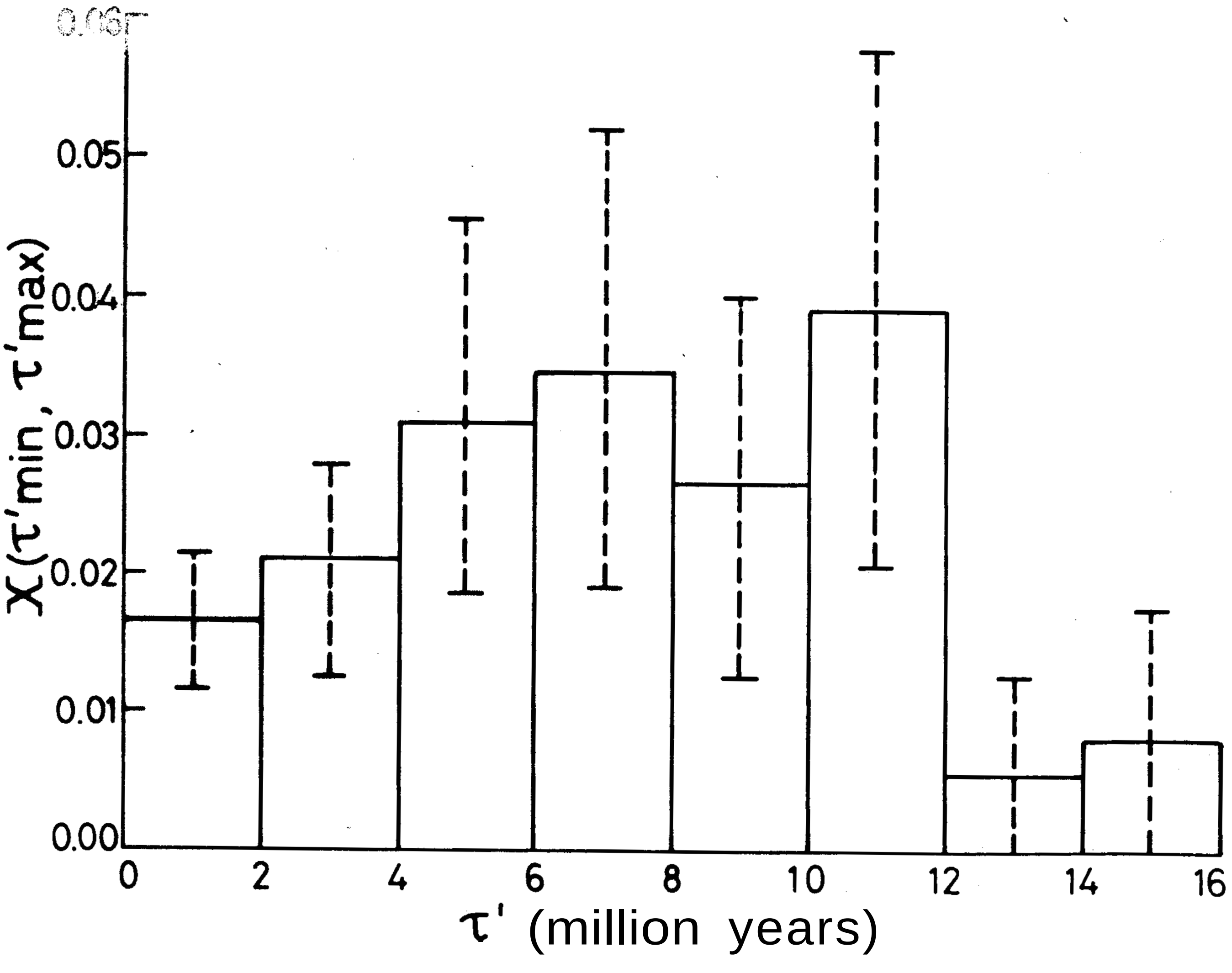

FIG. 5.3 Plot of modified pulsar current X against apparent age $\tau' = P/\dot{P}$. X has been averaged in τ' intervals of 2×10^6 years. There6 appears to be no apparent change in the current upto 12 x 10 years.

6 million years the current is constant, Incidentally, in terms of τ' injection occurs below $\sim 10^5$ years and can therefore be neglected in the discussion here.

Since the histogram in fig. 5.3 does not change right upto 12 million years, we can safely assume that the braking index remains constant in this range. Moreover, one can further conclude that there are no significant pulsar births or deaths in this range. by an argument similar to that in chapter 4 one can therefore arrive at the interesting result that $\bar{J}_{\tau',est}$ should be comparable to the birthrate b of pulsars. Since we have an independent estimate of b in section 5.3, we can therefore use eq. (5.11) to obtain an estimate of $\langle n \rangle$. We obtain $\langle n \rangle = 3.2^{+0.8}_{-0.7}$ where the error limits are the 95% confidence limits* It is interesting that our independent estimate of $\langle n \rangle$, based only on observational data, is fairly consistent with the dipole model value of $n = 3$. Incidentally, if we assume the death line of Ritchings (1976), it will be seen that, some of the high magentic field pulsars die at τ' values smaller than 12 million years. In that case $\bar{J}_{\tau',est}(0,12)$ would be smaller than b and the above value of $\langle n \rangle$ would be an overestimate, This strengthens the argument in favour of dipole braking in young pulsars.

The braking index has been measured independently only for the Crab pulsar (Groth 1975), yielding a value of 2.515. We do not consider this to be inconsistent with our result because by our reckoning the Crab belongs to a different class of pulsars, viz., the "un-injected" pulsars. Further, we have estimated the mean braking index for all pulsars as we have no information on the individual braking indices.

5.6 DISCUSSION

The main conclusions of this chapter are:

(1) The brithrate of pulsars is once every 16^{+3}_{-5} years in our Galaxy.

(2) A significant fraction of pulsars are born with initial periods > 0.45 s. If this "injection" of pulsars is due to neutron stars switching on as radio pulsars much later in their lives, then we can easily explain the lack of association between pulsars and supernova remnants* However, injection might just as well represent the range of initial periods of pulsars. In this case we conclude that the progenitors of pulsars lose a significant fraction of their angular momentum during the collapse into a neutron star.

(3) The mean braking index of pulsars is computed to be $\langle n \rangle = 3.2^{+0.8}_{-0.7}$. This is consistent with theoretical expectations.

The major source of uncertainty in this analysis is the luminosity model that we have assumed. However, the birthrate calculation is consistent with the result obtained in a model-independent manner (see chapter 4). Moreover, injection was already evident in the previous calculation* Therefore we believe that the luminosity model must be reasonabaly accurate.